Multimodal Imaging of Dental Pulp Healing Patterns Following Tooth Autotransplantation and Regenerative Endodontic Treatment

Mostafa EzEldeen,[†] Mariano N. Simon Pedano De Piero,[‡] Lianyi Xu,[*§] Ronald B. Driesen,[‖] Jan Wyatt,[†] Gertrude Van Gorp,[†] Nastaran Meschi,[¶] Bart Van Meerbeek,[#] Ivo Lambrichts,[‖] and Reinhilde Jacobs[***]*

SIGNIFICANCE

This study reports on dental pulp healing after tooth autotransplantation and regenerative endodontic treatment. Insights into patterns of reparative dentin formation can aid clinical decision-making for managing transplanted and immature teeth.

ABSTRACT

Introduction: Understanding the healing process of dental pulp after tooth autotransplantation (TAT) and regenerative endodontic treatment (RET) of immature teeth is important both clinically and scientifically. This study aimed to characterize the pattern of dental pulp healing in human teeth that underwent TAT and RET using state-of-the-art imaging techniques. **Materials and Methods:** This study examined 4 human teeth, 2 premolars that underwent TAT, and 2 central incisors that received RET. The premolars were extracted after 1 year (case 1) and 2 years (case 2) due to ankylosis, while the central incisors were extracted after 3 years (cases 3 and 4) for orthodontic reasons. Nanofocus x-ray computed tomography was used to image the samples before being processed for histological and immunohistochemical analysis. Laser scanning confocal second harmonic generation imaging (SHG) was used to examine the patterns of collagen deposition. A maturity-matched premolar was included as a negative control for the histological and SHG analysis. **Results:** Analysis of the 4 cases revealed different patterns of dental pulp healing. Similarities were observed in the progressive obliteration of the root canal space. However, a striking loss of typical pulpal architecture was observed in the TAT cases, while a pulp-like tissue was observed in one of the RET cases. Odontoblast-like cells were observed in cases 1 and 3. **Conclusions:** This study provided insights into the patterns of dental pulp healing after TAT and RET. The SHG imaging sheds light on the patterns of collagen deposition during reparative dentin formation. *(J Endod 2023;49:1058–1072.)*

KEY WORDS

Dental pulp healing; regenerative endodontic treatment; second harmonic generation imaging; tooth autotransplantation

From the *OMFS IMPATH Research Group, Faculty of Medicine, Department of Imaging and Pathology, KU Leuven and Oral and Maxillofacial Surgery, University Hospitals Leuven, Leuven, Belgium; †Department of Oral Health Sciences, KU Leuven (University of Leuven), KU Leuven and Pediatric Dentistry and Special Dental Care, University Hospitals Leuven, Leuven, Belgium; ‡Department of Oral Health Sciences, Endodontology, KU Leuven (University of Leuven), University Hospitals Leuven, KU Leuven, Leuven, Belgium; §Department of Stomatology, Tongji Hospital, Tongji Medical College, Huazhong University of Science and Technology, Wuhan, Hubei, China; ‖Biomedical Research Institute, Hasselt University, Diepenbeek, Belgium;

Tooth autotransplantation (TAT) and regenerative endodontic treatment (RET) are biologically-based dental treatments for the loss of dental tissue, mainly in children. The clinical evidence of pulp healing and continued root development after immature TAT has been repeatedly demonstrated[1-5]. These regenerative/reparative properties of the pulp/dentin complex after dental caries, attrition, restorative procedures, traumatic injuries and TAT[2,6] have contributed to the discovery of stem/stromal cells in the dental pulp[7] as well as the emergence of the idea of RET. From a tissue engineering point of view, TAT can be considered a model for stem/stromal cell transplantation[8-11], while RET can be regarded as a model for stem/stromal cell homing[12,13].

Existing knowledge regarding pulp-dentin complex healing after TAT originates mainly from the pioneering work of Andreasen et al, and Skoglund et al, in the late seventies and the early eighties on replanted and transplanted teeth in monkeys up to 9 months[14] and dogs for periods up to 6 months[15-17].

Dental pulp healing after tooth replantation was also studied in mice and rat models for up to 28 days, and these studies provided valuable insights into the immediate pulp response[18-21]. To the authors' knowledge, only 1 study reported on the pulpal response in humans after intentional tooth replantation of premolars, and this study was followed up to 6 months[22]. Despite these studies' important contributions, information is still lacking regarding the outcomes at longer periods, the re-establishment of innervation, and comprehensive characterization of the pulp response in an actual clinical situation where the tooth was transplanted to a different site.

RET has been associated with highly variable outcomes[23-25]. The histologic studies from animal and human teeth suggest that true pulp regeneration using the current protocol is difficult to achieve[25-28].

The main aim of the current study was to report on the outcomes of 2 cases of TAT and 2 cases of RET after 1–3 years. Moreover, we used state-of-the-art nano-focus computed tomography (CT), histological, immune-histochemical, and label-less confocal second harmonic generation (SHG) to gain insights into the different patterns of dental pulp healing.

MATERIALS AND METHODS

Ethical Approval and Informed Consent

For all samples included in this study, ethical approval was obtained by the local clinical trial center and by the commission for medical ethics of university hospitals and KU Leuven (S55287 and S54254). Informed (parental) consent was obtained.

¶Section of Endodontology, Department of Oral Health Sciences, Ghent University, Ghent, Belgium; #Department of Oral Health Sciences, KU Leuven (University of Leuven), BIOMAT - Biomaterials Research group & UZ Leuven, University Hospitals Leuven, Dentistry, Leuven, Belgium; and **Department of Dental Medicine, Karolinska Institute, Stockholm, Sweden

Address requests for reprints to Mostafa EzEldeen, Department of Imaging and Pathology, OMFS IMPATH Research Group, Faculty of Medicine, KU Leuven and Oral and Maxillofacial Surgery, University Hospitals Leuven, Leuven, Belgium.
E-mail address: mostafa.ezeldeen@kuleuven.be
0099-2399

https://doi.org/10.1016/j.joen.2023.06.003

Control Tooth

A mandibular left first premolar (tooth #21) removed for orthodontic reasons was retrieved from an 11 years-old girl while visiting the Department of Pediatric Dentistry, University Hospitals Leuven. This tooth served as a control for histological, immunohistochemical staining and label-less confocal SHG.

Case 1: Tooth Autotransplantation to a Dentoalveolar Trauma Site

A 10-year-old girl presented with an ankylosed maxillary right central incisor (tooth #8) after dentoalveolar trauma and subsequent root canal treatment (Fig. 1*A* and *B*). Replacement resorption was identified via cone-beam CT (CBCT) (Fig. 1*C–E*). After evaluating the prognosis, tooth #8 was extracted and replaced by the maxillary left second premolar (tooth #13) via CBCT-guided TAT[29] (Fig. 1*F–I*). Initial healing was observed for 3 months, after which orthodontic treatment was initiated.

However, 6 months post-TAT, the transplant was unresponsive to orthodontic forces and exhibited signs of ankylosis (Fig. 1*L* and *M*). Despite increased orthodontic forces, no improvement was observed after a year, necessitating extraction due to ankylosis (Fig. 1*N*). Yet, evidence of pulp healing was observed in the form of root canal obliteration and continued root development (Fig. 1*M*). The extracted tooth was then fixed in 4% paraformaldehyde for further examination via nano-focus CT and histological analysis.

Case 2: Tooth Autotransplantation to an Agenesis Site

A 10-year-old girl with multiple agenesis, including mandibular right second premolar (tooth #29), and mandibular left first and second premolars (teeth #21 and #20), was referred to our department (Fig. 2*A*). The decision was made to transplant the maxillary right second premolar (tooth #4) to the left mandibular region to aid orthodontic treatment (Fig. 2*B* and *C*). Orthodontic treatment began 6 months posttransplantation, with signs of periodontal and pulp healing observed until a year posttransplantation (Fig. 2*D-H*).

At 20 months post-TAT, however, the transplanted tooth displayed signs of ankylosis, including limited movement and a metallic sound on percussion (Fig. 2*I*). A low-dose CBCT scan revealed progressive replacement resorption on the root surface (Fig. 2*J* and *K*). The decision was made to keep the transplant as a bone anchor, but it was eventually extracted 24 months posttransplantation. The extracted tooth was preserved in 4% paraformaldehyde for further investigation.

Cases 3 &4: Regenerative Endodontic Treatment in 2 Teeth with Dentoalveolar Trauma

An eight-year-old girl arrived at our emergency clinic with dentoalveolar trauma, including a luxated maxillary left central incisor (tooth #9) and an avulsed maxillary right central incisor (tooth #8) (Supplemental Fig. S1A). Tooth #8 was repositioned and splinted (Supplemental Fig. S1B). Two weeks later, both central incisors underwent RET following a previously described protocol[23] (Supplemental Fig. S1C & D). A 2.5-year post-RET follow-up showed successful treatment with no signs of inflammation and progressive root canal obliteration (Supplemental Fig. S1E–M).

Three years post-RET, the 2 central incisors and 2 lower premolars were extracted as part of orthodontic treatment. The extracted teeth (#8 and #9) were preserved in 4% paraformaldehyde for further analysis. Maxillary lateral incisors were orthodontically moved to fill the central incisor space and were given esthetic build-ups (Supplemental Fig. S1N & O).

Nano-focus X-ray Computed Tomography

CT images were acquired on a submicrometric resolution CT device (Nanotom, GE Phoenix, Blomberg, Germany). Detailed imaging protocol is provided in Supplemental materials S1.1.

Image Processing and 3D Analysis

Pre-operative CBCT and nano-CT scans were analyzed as detailed in Supplemental S1.2.

Histological Processing

Histological processing was performed as detailed in Supplemental S1.3.

Immunostaining

Immunostaining was performed as detailed in Supplemental S1.4.

Second-harmonic Generation Imaging

SHG imaging protocol and processing are detailed in Supplemental S1.5.

RESULTS

The typical morphology of the pulp-dentin complex, as observed in various imaging techniques and staining, including SHG imaging, is shown in Figure 3. The measurements from 3D analysis for the hard tissue change and the main histological findings are summarized in Table 1.

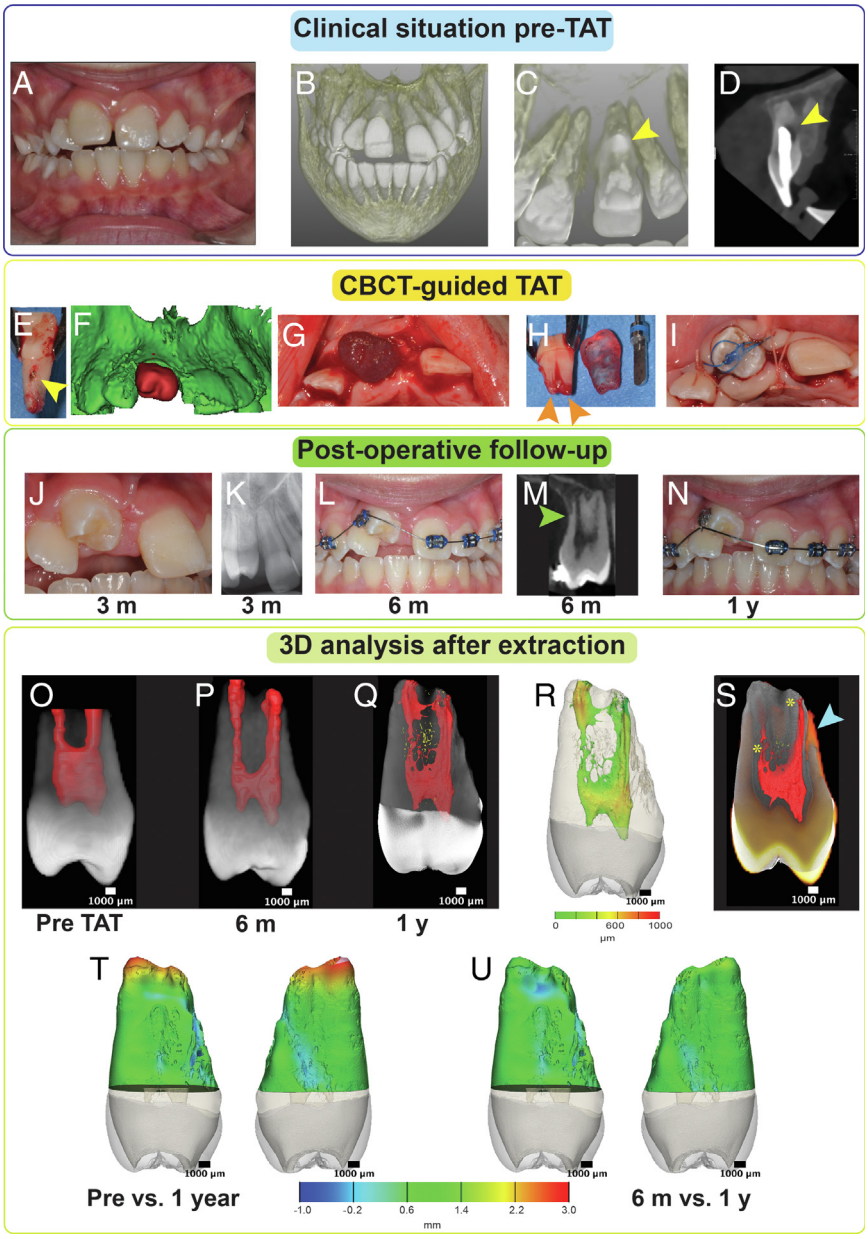

FIGURE 1 – Case 1 (TAT), (*A, B*) clinical and radiological presentation of ankylotic tooth #8, (*C, D*) root resorption at the palatal surface (*yellow arrowheads*), (*E*) confirmation of the resorption lesion after extraction, (*F-I*) the surgical process of CBCT-guided TAT, (*H*) intact apical papilla at TAT (orange arrowheads), (*J-N*) clinical and radiological follow-up till 1-year post-TAT, (*M*) detection of ankylosis and replacement resorption at 6 months post-TAT, (*O-Q*) 3D reconstruction of the transplanted tooth from CBCT scans pre-TAT (*O*), at 6 months post-TAT (*P*), and from the nano-CT scan at 1-year post-TAT (*Q*). (*R*) color coded map for the root canal system thickness (mean= 269.4 µm ±381.7), (*S*) superimposition of the pre-TAT image (in orange color) on the nano-CT image 1-year post-TAT (in grey values) showing the extent of root resorption (blue arrowhead) and highlighting the newly formed dentin post-TAT (*yellow asterisks*), (*T*) surface distance map for root tissue change post-TAT, the root surface resorption extended to -853.5 µm, while the hard tissue gain extended to 3238.6 µm (mean = 333.5 µm) at 1 year post-TAT, (*U*) between 6 months and 1 year post-TAT, the root surface resorption extended to -1289.1 µm, while the hard tissue gain extended to 1276.1 µm (mean= -26.4 µm). CT, Computed tomography; TAT, Tooth autotransplantation.

Case 1: Dental Pulp Healing after TAT to a Dentoalveolar Trauma Site

The 3D measurements indicate significant root canal space obliteration and root maturation in the initial 6 months post-TAT, with substantial root surface resorption in the final 6 months before extraction. Post-TAT dentin formation is demarcated by a calciotraumatic line, visible in both the nano-CT scan and histological sections (Fig. 4*A-C*). The coronal third of the root shows a striking loss of the typical pulp architecture, replaced by cell-poor, vascularized fibrous connective tissue with dense collagen organization (Fig. 4*D*). The newly formed dentin resembles reparative dentin, with no predentin present. A nestin-positive odontoblast-like cell layer lines the interface between dentin and the pulp tissue (Fig. 4*G-I*). Mineralization foci, weakly stained for nestin, contain cells that seem to originate from the blood vessel walls (Fig. 4*D*, *E* and *H*). This is further observed in the SHG imaging as they are characterized by a strong two-photon autofluorescence signal typical for cells (Fig. 4*F*).

The middle third of the root reveals less tubular dentin with cell-containing lacune-like structures and altered collagen deposition patterns (Fig. 5*D* and *E*). The pulp is vascularized with few cells within the extracellular matrix (Fig. 5*H* and *I*), and zones of dense collagen-rich fibers (Fig. 5*F*). Odontoblasts are present at the interface, extending into the dentin without a predentin layer (Fig. 5*H* and *K*). Patterns of hard tissue deposition and pulp healing at the apical third are shown in Supplemental Figure S2.

Case 2: Dental Pulp Healing after TAT to an Agenesis Site

The nano-CT scan and the histological sections showed a calciotraumatic line marking the tissue formation post-TAT. The root canal space was filled with porous bone-like tissue with cells containing lacunes (Fig. 6*A-F*) at the coronal and middle thirds containing neurofilament-positive cells (Fig. 6*G*). In addition, the interface between the primary root dentin and the newly formed tissue exhibited highly disordered collagen organization with cell-containing lacunes, as seen through SHG imaging (Fig. 6*H*).

At the apical third, remnants of the root canal system showed pulp tissue (Fig. 6*I* and *J*) containing several fibroblasts at its core and neurovascular bundles surrounded by $CD90^{+}$ cells (Fig. 6*M* and *N*). It is worth noting that the cells lining the dentin wall at the apex appeared parallel to the dentin and not perpendicular to it (Fig. 6*L*). Overall, these observations show tissue regeneration and repair combinations post-TAT, accompanied by notable changes in the root canal system and surrounding hard tissue.

Case 3: Healing after RET in a Luxated Incisor

Following RET, observations showed distinct porosities and patches of dense mineralized tissue within the newly formed tissue from the

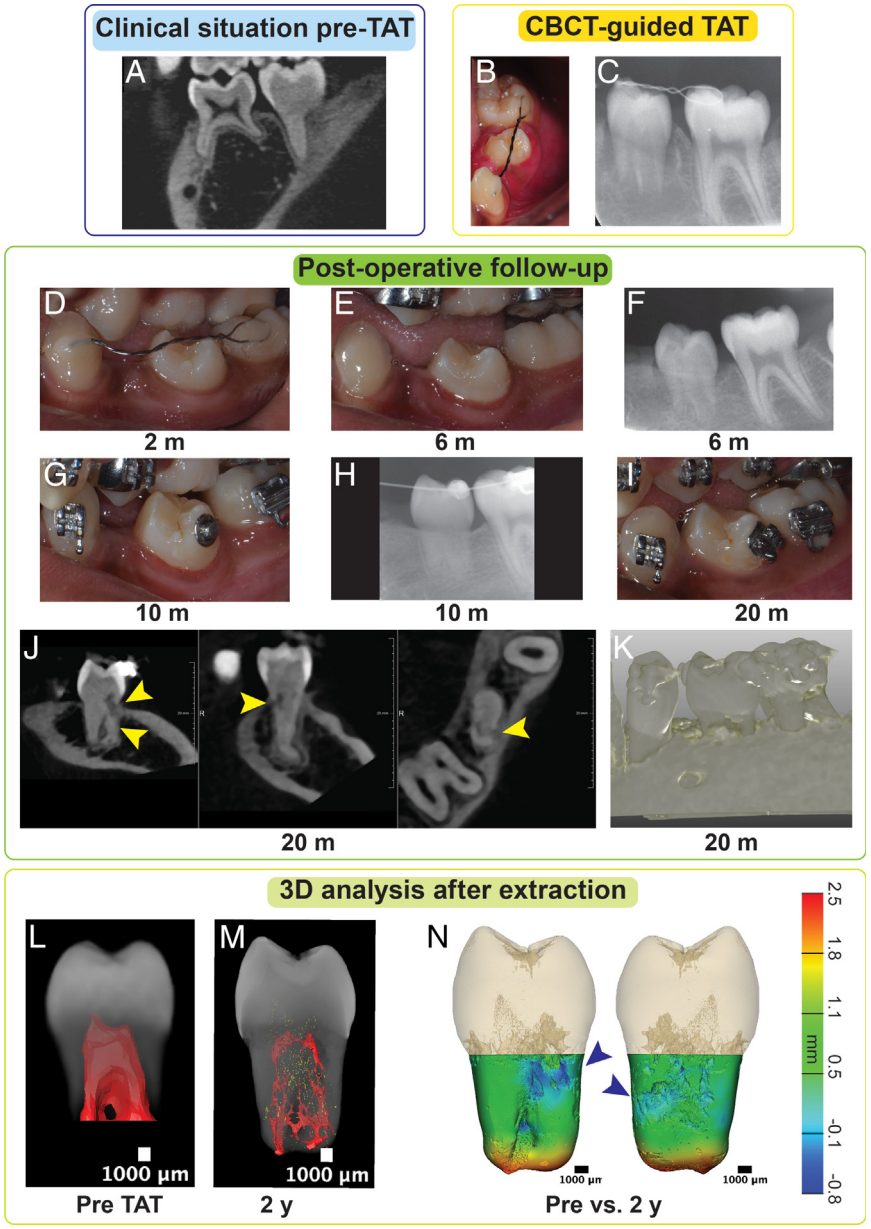

FIGURE 2 – Case 2 (TAT), (*A*) a 10-year-old girl with agenesis of the 2 premolars, (*B-C*) directly after TAT of tooth #4 to the site of tooth 20, (*D-I*) clinical and radiological follow-up till 20 months post-TAT, (*J, K*) detection of ankylosis and replacement resorption at 20 months post-TAT, (*L, M*) 3D reconstruction of the transplanted tooth and root canal system from CBCT scans pre-TAT (*L*), and from the nano-CT scan at 2 years post-TAT, (*N*) surface distance maps for root tissue change post-TAT. CBCT, Cone-beam computed tomography; CT, Computed tomography; TAT, Tooth autotransplantation.

middle third of the root to the calcium silicate cement. Nano-CT images and histological sections confirmed post-RET hard tissue formation, marked by a calciotraumatic line (Fig. 7*A*, *C* and *D*).

The transition from primary dentin to newly formed tissue revealed mineralized tissue with lacuna-like structures (Fig. 7*C*, *D* and *H*), surrounded by dense collagen deposits as shown by SHG imaging (Fig. 7*H*). Toward the root canal space, a transition to tubular dentin-like tissue occurred (Fig. 7*E*), with a slight deviation in collagen deposition direction from the primary dentin (Fig. 7*H*).

Inside the root canal space, a de-novo pulp-like tissue, free of inflammation and populated with cells and neurovascular bundles, was observed (Fig. 7*E* and *G*). Notably, nestin-positive odontoblast-like cells lined the newly formed dentin interface, extending processes into dentin tubules (Fig. 7*F*). This nestin staining gradient mirrored the control tooth's (Fig. 7*C*).

Figure 8 presents sections toward the middle third of the root, showing similar tissue formation patterns to the apical third (Fig. 8*B–L*). The transition from primary to reparative dentin housed $CD90^+$ cells within lacunae (Fig. 8*E* and *J*) and dense collagen patches were observed, followed by an intertubular collagen deposition pattern almost parallel to the primary dentin (Fig. 8*H*).

Case 4: Healing after RET in an Avulsed Incisor

Post-RET nano-CT images revealed partial filling of the apical third root canal space with newly formed hard tissue after 3 years (Fig. 9*A*, *C* and *D*). This included a thin, interconnected 3D root canal system, patches of dense mineralized tissue, and distinct porosities unconnected to the root canal system (Fig. 9*A* and *B*). Material remnants, presumably from the procedural collagen sponge, were noted separating the new hard tissue from the calcium silicate cement (Fig. 9*A* and *E*).

The apical third of the root canal was filled with porous tissue resembling bone or cementum (Fig. 9*A*, *C*, *D*, *H* and *I*). It featured lacunes filled with connective tissue and blood vessels (Fig. 9*G* and *K*). The transition from primary root dentin to the new tissue, as seen via SHG imaging, showed highly disordered collagen organization (Fig. 9*I* and *J*). Cellular inclusions were also in the new hard tissue (Fig. 9*L* and *M*). Notably, no pulp-like tissue was identified within the root canal system.

DISCUSSION

The healing capacity of the pulp-dentin complex is a fascinating process that is not yet fully understood. For TAT, the mainstream theory is that the pulp tissue will undergo a process of sterile necrosis followed by replacement by new tissue[15]. The healing process could also involve invading periodontal ligament-derived stromal cells accompanied by cementum deposition on the root canal walls or bone invasion[14,16,30]. This process is supported by revascularization, reaching the entire length of the pulp 30 days postreplantation or transplantation[17]. However, it was not shown when this process started precisely. The exact mechanism of this revascularization is highly speculative and end-to-end anastomoses of the existing vasculature were hypothesized[17]. Moreover, this process should involve the immune system through the infiltration of neutrophils

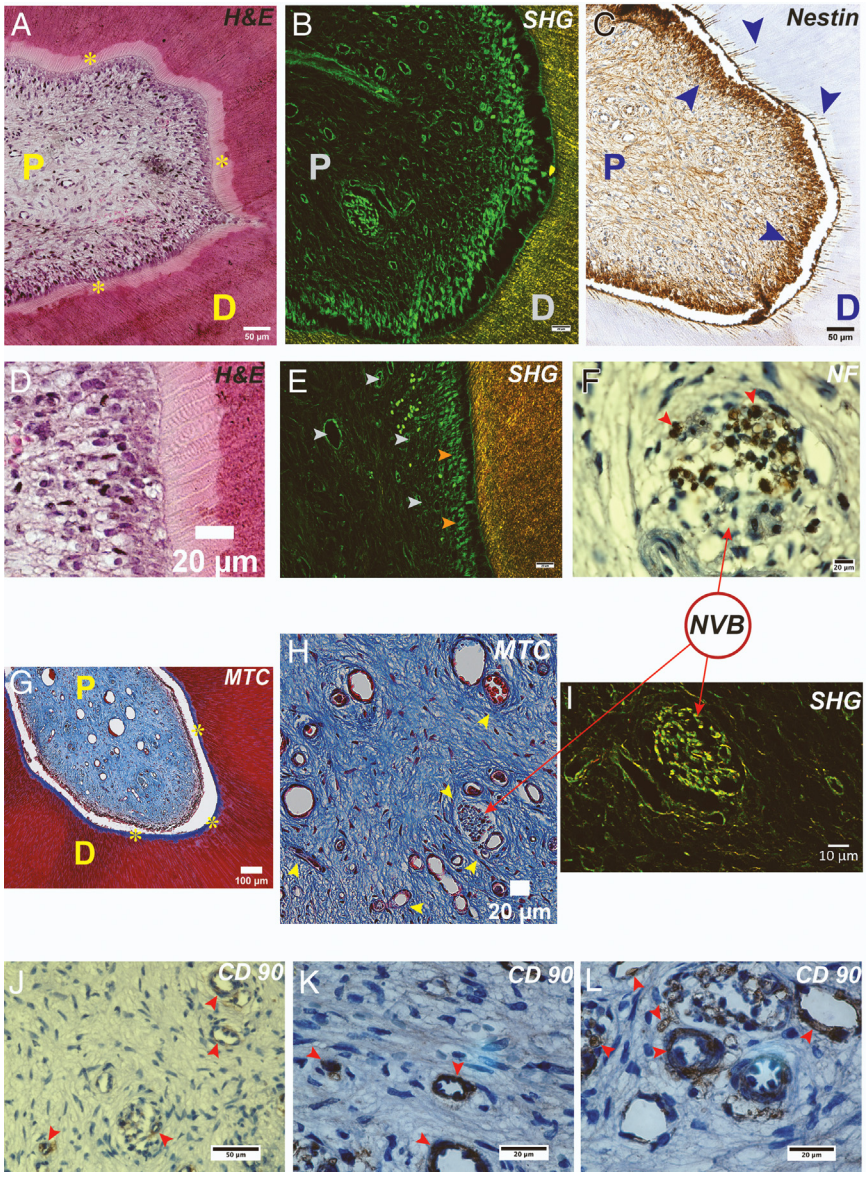

FIGURE 3 – Morphology of the pulp-dentin complex from a maturity matched premolar as seen in different stains and imaging modalities, (*A*) hematoxylin and eosin (H&E) staining, dentin (D), pulp (P), and predentin (*yellow asterisks*), (*B*) second harmonic generation (SHG) label-less visualization of collagen and general tissue architecture, yellow is forward SHG signal indicating mainly collagen I showing an intense signal corresponding to intertubular dentin, red is backward SHG signal, green is 2-photon autofluorescence showing the fibrous architecture of the pulp, (*C*) nestin immunostaining showing an typical intense brown staining at the odontoblast layer as well as the processes that are extending through the predentin into the dentin (blue arrowheads), (*D*) H&E staining showing the organization of the odontoblasts, (*E*) SHG imaging showing the organization of the odontoblasts (orange arrowheads), extending their processes into the dentinal tubules that are surrounded by intertubular collagen (yellow & red color), while supported by a network of blood vessels in different sizes (gray arrows), (*F*) neurofilament (NF) immunostaining, (*G*) Masson'strichrome (MTC) staining, dentin (D), pulp (P), and predentin (yellow asterisks), (*H*) MTC staining highlighting the neurovascular bundles (yellow arrowheads) inside the dental pulp, (*I*) SHG imaging showing a neurovascular bundle inside the dental pulp, (*J-L*) CD90 immunostaining, $CD90^{+}$ cells only present in the vicinity of the vasculature. Note the morphology of the neurovascular bundle (NVB) can be recognized clearly on MTC and SHG corresponding to NF immunostaining.

followed by macrophages to eliminate the necrotic cells and be followed by a shift from inflammation to repair/regeneration to achieve a healed pulp. Prior studies did not fully explain the mechanism of new pulp tissue formation and the source of cells repopulating the pulp[15-17].

Current evidence regarding the apical papilla shows it to be the driving force behind tooth root growth and maturation. Stem cells of the apical papilla (SCAPs) show the capacity to differentiate into odontoblasts and adipocytes. Moreover, SCAPs have shown a higher proliferative, migratory, and mineralized matrix deposition compared to dental pulp stem/stromal cells (DPSCs)[31]. It is hypothesized that SCAPs might be the source of primary odontoblasts that form the primary dentin of the tooth root[32], while DPSCs are the source of the cells replacing odontoblasts and producing reparative dentin[7]. Therefore, in the mainstream hypothesis that all cells within the pulp are replaced by new cells, these new cells might originate from the apical papilla.

A second hypothesis, originating from tooth replantation studies in small animal models, suggests the involvement of immunocompetent cells in replacing the degenerated odontoblast layer to form odontoblast-like cells capable of producing

TABLE 1 - Summary of the Measurements From 3D Analysis for the Hard Tissue Change and the Main Histological Findings

	Case 1 (at 1 y)	Case 2 (at 2 y)	Case 3 (at 3 y)	Case 4 (at 3 y)
3D analysis metrics				
Hard-tissue change*	+54.5 mm^3 (+33.5 %)	+47.9 mm^3 (+46.4%)	Not available	Not available
Root-surface resorption	−853.5 μm	−794.6 μm	Not available	Not available
Mean thickness of the root canal system	269.4 μm ± 381.7	102.8 μm ± 82.2	82.1 μm ± 63.3	61.6 μm ± 33.2
Histological findings				
Vascularized pulp tissue	Present	Present only in the apical third	Present	Not present
Odontoblast like cells ($nestin^+$)	Present	Not present	Present	Not present
Collagen deposition with newly formed hardtissue	Organized	Not organized	Combination of organized and not organized	Not organized

*Measured from the cementoenamel junction to the root apex.

reparative dentin[33,34]. Class II major histocompatibility complex antigen-presenting cells in the dental pulp plays a significant role in response to stress or bacterial invasion[35]. major histocompatibility complexantigen-presenting cells are in the sub-odontoblast layer and the vicinity of the blood vessels in the pulp[33-35]. Heat shock protein 25, highly expressed in the odontoblasts[19], is thought to be released upon stress conditions such as hypoxia, typical after TAT, recruiting antigen-presenting cells to the site of injury[33]. Furthermore, evidence from the *ex-vivo* tooth model studies suggests that DPSCs survive up to 4 weeks inside the pulps of extracted immature wisdom molars when suspended in a culture medium[36]. After an induced injury to the odontoblasts, DPSCs migrated from the vicinity of the blood vessels to form reparative dentin[37-39]. Therefore, it might be possible that not all cells inside the pulp will degenerate after TAT. Furthermore, other cell populations, such as immune cells or dental pulp stromal cells, could migrate from their niches to form a de-novo odontoblast layer along the root canal walls.

In the current report, the pulpal healing patterns within the 2 TAT cases were different. In the first case, the reparative dentin formation appeared to originate from the canal walls toward the center of the pulp, with an odontoblast-like cell layer at the interface with the pulp tissue. In the second case, the healing can be described as lamellar arranged hard tissue along the dentinal wall, progressively filling the root canal to the apical third without an odontoblast-like layer. In the first case, loss of typical pulp architecture can be observed with mineralization foci that seem to originate from the pulp's core from the blood vessels. In the second case, pulp-like tissue could be observed at the most apical part of the root. It is possible that the difference is related to the period post-TAT (1 year vs 2 years) and that the pulp of case 1 will resemble case 2 at the coronal and middle thirds when it is completely obliterated at 2 years. Our observations align with the observations from the replantation and transplantation studies in large animal models[14,16]. Skoglund et al, observed a pulp with a typical morphologic structure only in 2 out of 15 teeth 6 months postreplantation/transplantation of dogs' incisors[16]. In the other 13 teeth, the pulp was described as connective tissue deficient in cells and blood vessels and devoid of odontoblasts.

Furthermore, the pulp space contained large cells containing hard tissue deposits in addition to the accumulation of macrophages[16]. However, it must be noted that no immunostaining was performed in that study. In the current report, a nestin-positive odontoblast-like cell layer was observed at the boundary of the pulp. Nestin is expressed only in functional and differentiated odontoblasts[40,41]. Moreover, nestin expression is upregulated in odontoblasts surrounding injury sites to respond by laying down reparative dentin[37,38,40]. Whether these cells migrated from the apical papilla, immunocompetent cells or DPSCs migrating from the core of the pulp, they have differentiated into functional odontoblasts and secreted dentin. Fiane et al, reported histological outcomes of replanted immature and mature premolars in humans[22]. In both immature and mature premolars, an initial degeneration of the odontoblast layer and loss of vasculature and typical pulp structure was observed after 3 weeks.

Further, revascularization and reparative dentin formation in the immature teeth were evident after 6 weeks. After 6 months, complete pulp obliteration in the coronal part was observed with traces of pulp tissue with a typical architecture, including a predentin layer[22]. In our study, we did not observe a predentin layer.

Kristerson et al reported extensive dentin formation after revascularization of replanted incisors in monkeys after 9 months. The average daily dentin formation was 4 μm, measured from histology sections[14]. The current report observed a 34% and 48% gain in root hard tissue volume starting from the cementoenamel junction after 1 year and 2 years, respectively. It was hypothesized that this accelerated dentin production is because of a loss of pulp tissue's autonomic and/or sensory nervous control[14,30].

The RET-treated teeth in cases 3 & 4 demonstrated a successful clinical outcome at 3 years. Nano-CT analysis showed that the newly formed tissue consisted of regions of different intensities and porosities, suggesting a heterogeneous nature of the formed tissue. This contrasts with previous reports on RET using μCT imaging, where the newly formed tissue had a similar appearance to the native dentin[27]. Our studies using hematoxylin and eosin, SHG, and immunostaining showed that the newly formed tissues in case 3 represented osteodentin and dentin-like tissue with a distinct organization. The osteodentin was formed at the interface with the primary dentin, followed by a de-novo reparative tubular dentin toward the pulp.

Moreover, the newly formed dentin in case 3 was lined with functional odontoblast-like cells. The core of the newly formed pulp showed a well-established vasculature. This is a unique finding, as most of the previous reports on RET showed the formation of cementum-like tissue and unorganized mineralized tissue along the walls of the root canal with fibrous connective tissue without odontoblast-like cells[42-44]. Austah et al, showed the presence of odontoblast-like cells lining the newly formed dentin[27]. However, this was slightly different from the current report as the newly formed dentin was continuous with the primary dentin and had similar density and

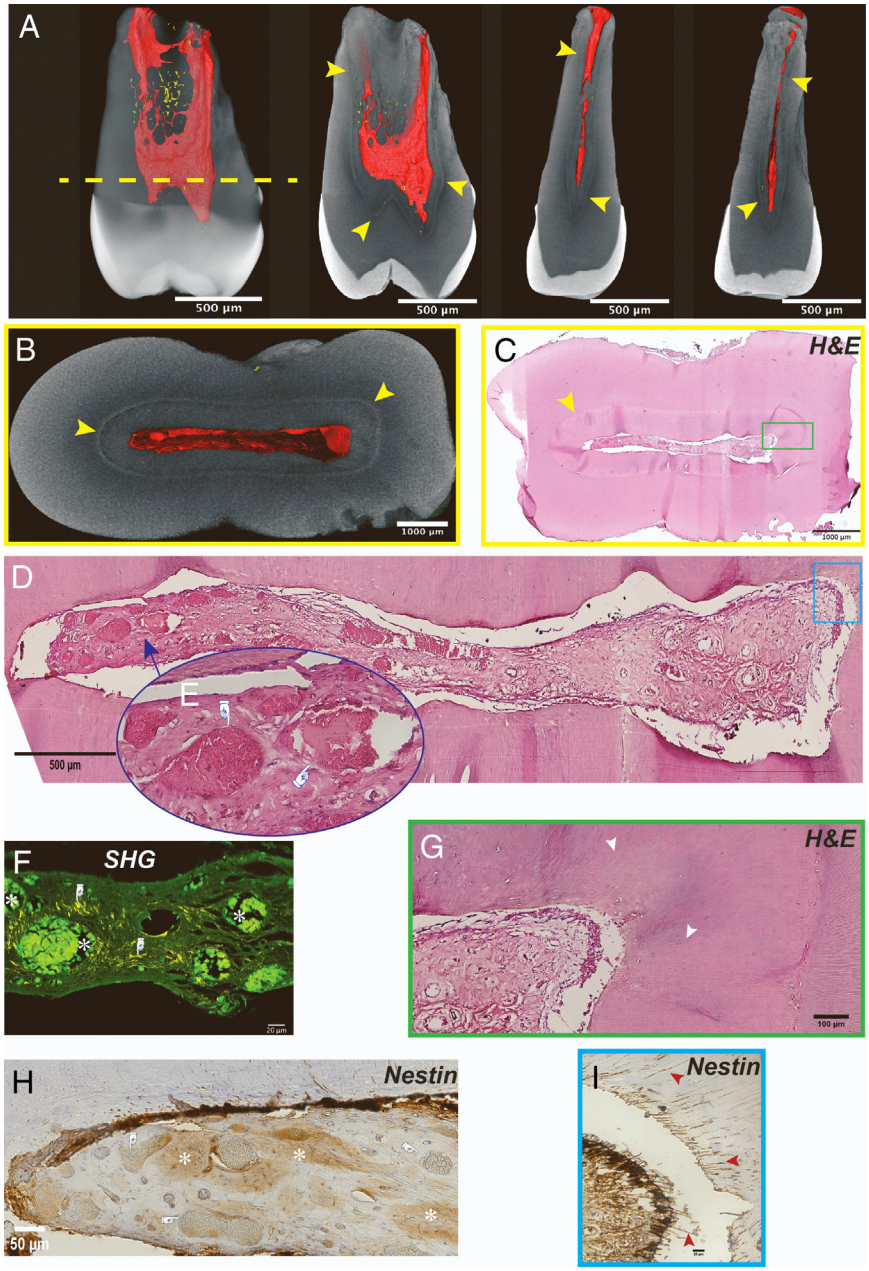

FIGURE 4 – Case 1 (TAT), multimodality imaging for the pattern of pulp healing 1-year post-TAT. (*A*) 3D reconstruction of the transplanted tooth from the nano-CT scan 1 year post-TAT, and longitudinal sections showing the calciotraumatic line defining dentin formation post-TAT (*yellow arrowheads*), (*B*) nano-CT cross-section at the coronal third of the root corresponding to the dashed yellow line in (*A*), newly formed dentin originated from the canal walls (*yellow arrowheads*) toward the center of the pulp, (*C*) H&E stained section corresponding to (*B*), (*D*) healed pulp tissue 1-year post-TAT, (*E*) magnification for the section in D (blue arrow) showing progressive mineralization within the pulp, (*F*) SHG imaging for an area corresponding to (*E & H*) showing that the mineralization foci have a low collagen content (*white asterisks*), while patches of dense collagen are seen scattered over the pulp (pointing hand). (*G*) magnification for the green rectangle in (*C*) showing the structure of the healed pulp and the newly formed tubular reparative dentin (*white arrow heads*), (*H*) nestin immunostaining in an area corresponding to (E) showing patches of nestin positive staining (*white asterisks*), while the mineralization foci are weakly stained for nestin (pointing hand), (*I*) nestin immunostaining in an area corresponding to the blue rectangle in (*D*) showing a nestin positive functional odontoblast layer with processes extending into the dentin (*brown arrowheads*).CT, Computed tomography; SHG, Second harmonic generation; TAT, Tooth autotransplantation.

organization of tubules. In our study, the newly formed dentin resembled tertiary reparative dentin with fewer tubules and aligned odontoblasts.

In contrast to case 3, the tissue formed post-RET in case 4 could only fill one third of the root canal. The hard tissue formed along the canal walls with connective tissue inclusions and blood vessels, similar to the organization of bone or cementum rather than dentin. This finding aligns with several previous reports on RET[42-44]. The main difference between cases 3 and 4 is the type of trauma; there was luxation in case 3 and complete avulsion in case 4. The difference in the outcome might be due to the survival of the apical papilla cells in case 3 in contrast to case 4.

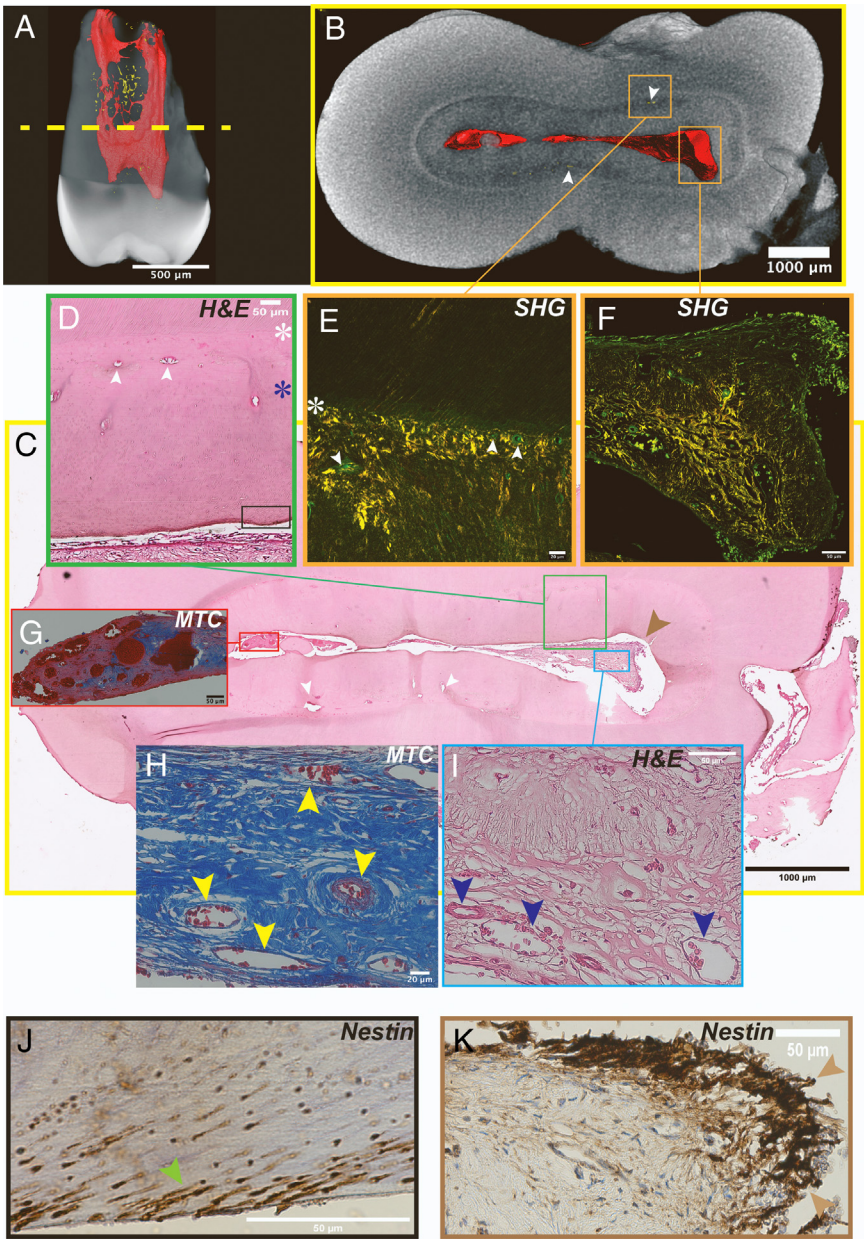

FIGURE 5 – Case 1 (TAT), (*A*) 3D reconstruction of the transplanted tooth from the nano-CT scan 1-year post-TAT, (*B*) nano-CT cross-section at the middle third of the root corresponding to the dashed yellow line in (*A*), porosities at the transition from primary to newly formed dentin (white arrowheads), (*C*) H&E stained section corresponding to (*B*), (*D*) the transition from primary tubular dentin to atubular reparative dentin (*white asterisk*) then the transition to tubular reparative dentin (*blue asterisk*) running to the pulp, (*E*) SHG imaging for the interface between primary and reparative dentin showing cell containing lacunes (*white arrowheads*) at the transition (*white asterisk*) surrounded by patches of nonuniform collagen deposition (intense yellow signal) in contrast to an organized collagen deposition in the tubular reparative dentin zone, (*F*) SHG imaging showing the architecture of the healed pulp and dense collagen I deposition at the center (intense forward SHG signal in *yellow color*), (*G*) progressive mineralization within the pulp demonstrated by MTC staining, (*H & I*) vascularization within the core of the pulp (yellow and blue arrowheads), (*J*) magnification of the black rectangle in (*D*) showing positive nestin staining inside the dentinal tubules (green arrowhead), (*K*) pattern of nestin immunostaining in the healed pulp in area corresponding to the brown arrowhead in (*C*), note the positive stained odontoblast processes (*brown arrowheads*). CT, Computed tomography; H&E, hematoxylin and eosin; SHG, Second harmonic generation; TAT, Tooth autotransplantation.

The cells involved in pulp healing/regeneration in RET are thought to originate from the apical papilla, under the condition that it will survive the initial insult causing pulp necrosis[12,45]. Conditioning the root canal walls to release the growth factors trapped in the dentin and induction of bleeding into the root canal is hypothesized to provide a blood clot scaffold enriched with growth factors to induce SCAPs migration and subsequent differentiation into odontoblasts[12,13,27,43,45]. Although the RET outcomes are highly variable clinically[24,46] and histologically[25,27,42-44,47,48], they provide valuable insights into the pulp repair and regeneration mechanisms.

The progressive root canal obliteration and the nonuniform tissue formation after RET may result from the lack of an exogenous

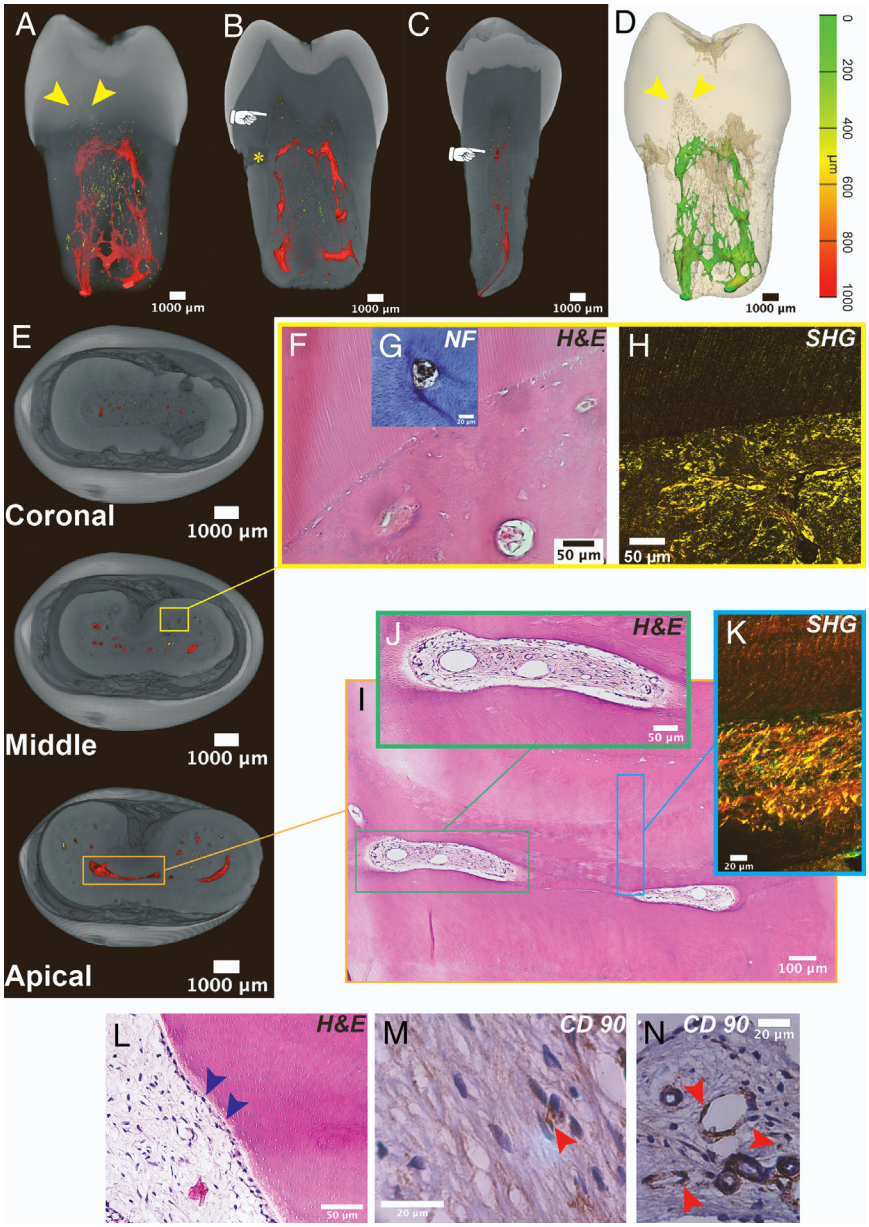

FIGURE 6 – Case 2 (TAT), multimodality imaging for the pattern of pulp healing 2 years post-TAT, (*A*) 3D reconstruction of the transplanted tooth from the nano-CT scan 2 years post-TAT, original pulp chamber outline (*yellow arrowheads*), (B, *C*) longitudinal sections showing the calciotraumatic line defining dentin formation post-TAT (pointing hand), and resorption lacunes (*yellow asterisk*), (*D*) color coded map for the root canal system thickness (mean = 102.8 µm ± 82.2), newly formed hard tissue is marked by high porosity (*yellow arrowheads*), (*E*) nano-CT cross-sections from the coronal, middle and apical thirds of the root demonstrating the nature of the newly formed hard tissue, (*F*) the interface between primary dentin and newly formed hard tissue, (*G*) tissue inside the lacunae within newly formed hard-tissue tissue stain positive for neurofilament (NF), (*H*) SHG imaging for the interface showing the difference in the collagen deposition pattern, (*I*) traces of the root canal system at the apical third, (*J*) loose connective pulp-like tissue within the canal in the apical third, (*K*) different patterns of collagen deposition varying between organized inter-tubular collagen to un-organized dense collagen deposits surrounding cell containing lacunes, (*L*) pulp-like tissue at the apex, note the parallel orientation of the cells lining the dentin wall (*blue arrowheads*), (*M & N*) pulp like tissue with several fibroblasts at its core and vascular bundles surrounded by CD 90 positive cells (*red arrowheads*). CT, Computed tomography; SHG, Second harmonic generation; TAT, Tooth autotransplantation.

scaffold providing the appropriate guidance for cell/tissue organization[27]. However, the same progressive obliteration is observed after TAT, where a nature-engineered pulp scaffold is present. Therefore, additional research is needed to elucidate the molecular mechanisms controlling odontogenesis and the pulp-dentin complex's healing. The application of RNA and single-cell sequencing in well-designed animal studies and tissue samples might unravel novel key molecules involved in the process.

This study utilized nanofocus CT and SHG imaging to shed new light on dental pulp healing after TAT and RET. Nanofocus CT allowed for the 3D visualization and quantification of the root canal systems and the new hard tissues formed, while SHG

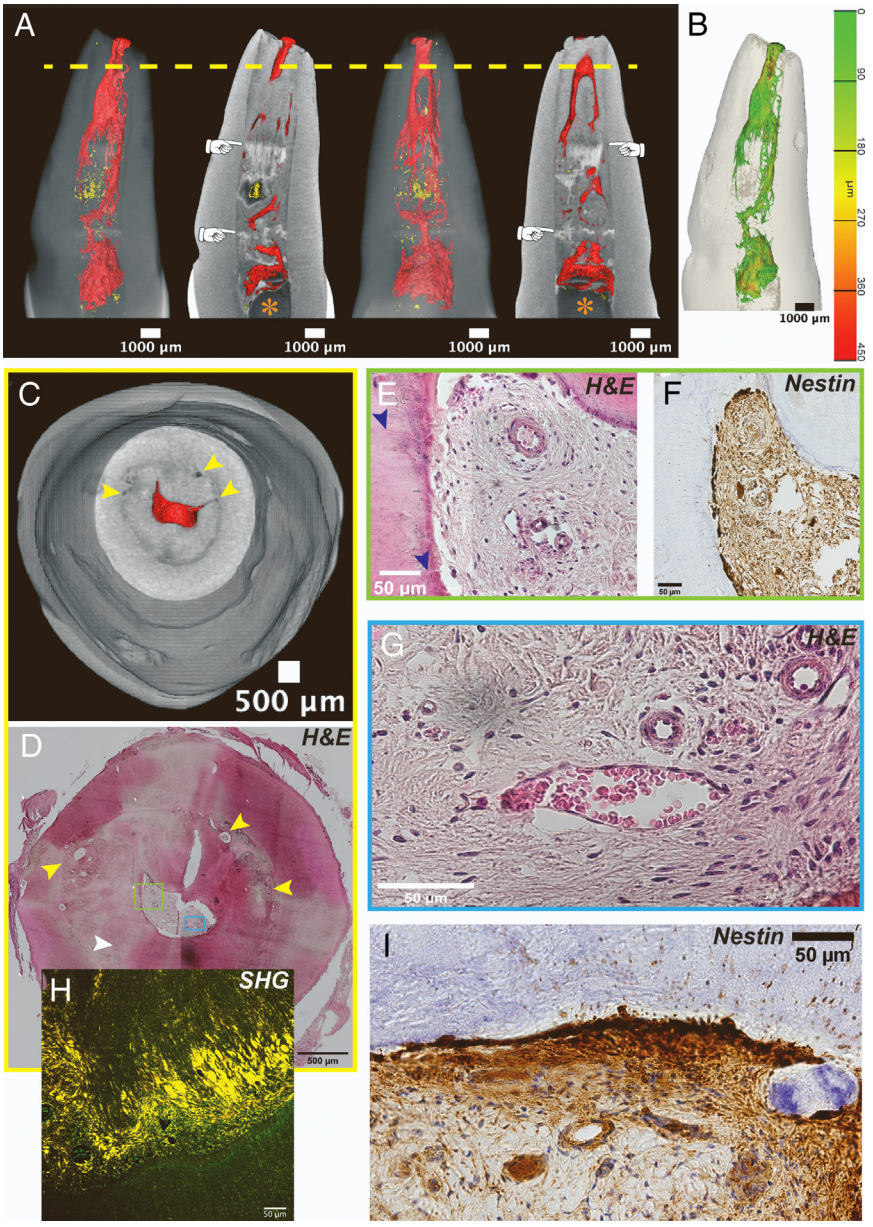

FIGURE 7 – Case 3 (RET), multimodality imaging for the pattern of pulp healing 3 years post-RET, (*A*) 3D reconstruction of tooth #9 from the nano-CT scan 3 year post-RET, note the 3D interconnected root canal system (in *red*) and the porosity inside newly formed tissue (in *yellow*) and longitudinal sections showing the calciotraumatic line defining hard tissue formation post-RET showing zones of different intensities and porosities (pointing hands), (*B*) color-coded map for the root canal system thickness (mean = 82.1 µm ± 63.3). (*C*) nano-CT cross-section at the apical third of the root corresponding to the dashed yellow line in (*A*), (*D*) H&E stained cross-section corresponding to (*C*), showing different patterns of hard tissue deposition (yellow and white arrowheads), (*E*) magnification for the green square in (*D*) showing vascularized pulp-like tissue lined by tubular reparative dentin (*blue arrowheads*), (*F*) nestin immunostaining for an area corresponding to (*E*) showing nestin positive odontblast-like cells lining the newly formed dentin, (*G*) magnification for the blue rectangle in (*D*) showing neurovascular bundles in different sizes and fibroblasts within the core of the newly formed pulp tissue, (*H*) SHG imaging for the interface between primary dentin and reparative dentin showing cell containing lacunes surrounded with dense collagen deposition followed by inter-tubular collagen deposition that has a similar deposition direction to the collagen in the primary dentin, (*I*) pattern of nestin immunostaining within the newly formed pulp, note the absence of the predentin. RET, regenerative endodontic treatment; CT, Computed tomography; H&E, hematoxylin and eosin; SHG, Second harmonic generation; TAT, Tooth autotransplantation.

imaging offered a unique, label-free perspective on collagen organization. These insights are valuable for understanding tissue regeneration and repair.

Finally, from a clinical point of view, the type of pulpal healing outcomes, as reported in the current study, are highly desirable and result in a more robust tooth root structure that approximates normal dental pulp. Moreover, they bring us 1 step closer to the inspired aim of a biological tissue engineering-based treatment modality.

CONCLUSION

This study provided insights into the patterns of dental pulp healing after TAT and RET. The SHG imaging sheds light on the patterns of collagen deposition during reparative dentin formation.

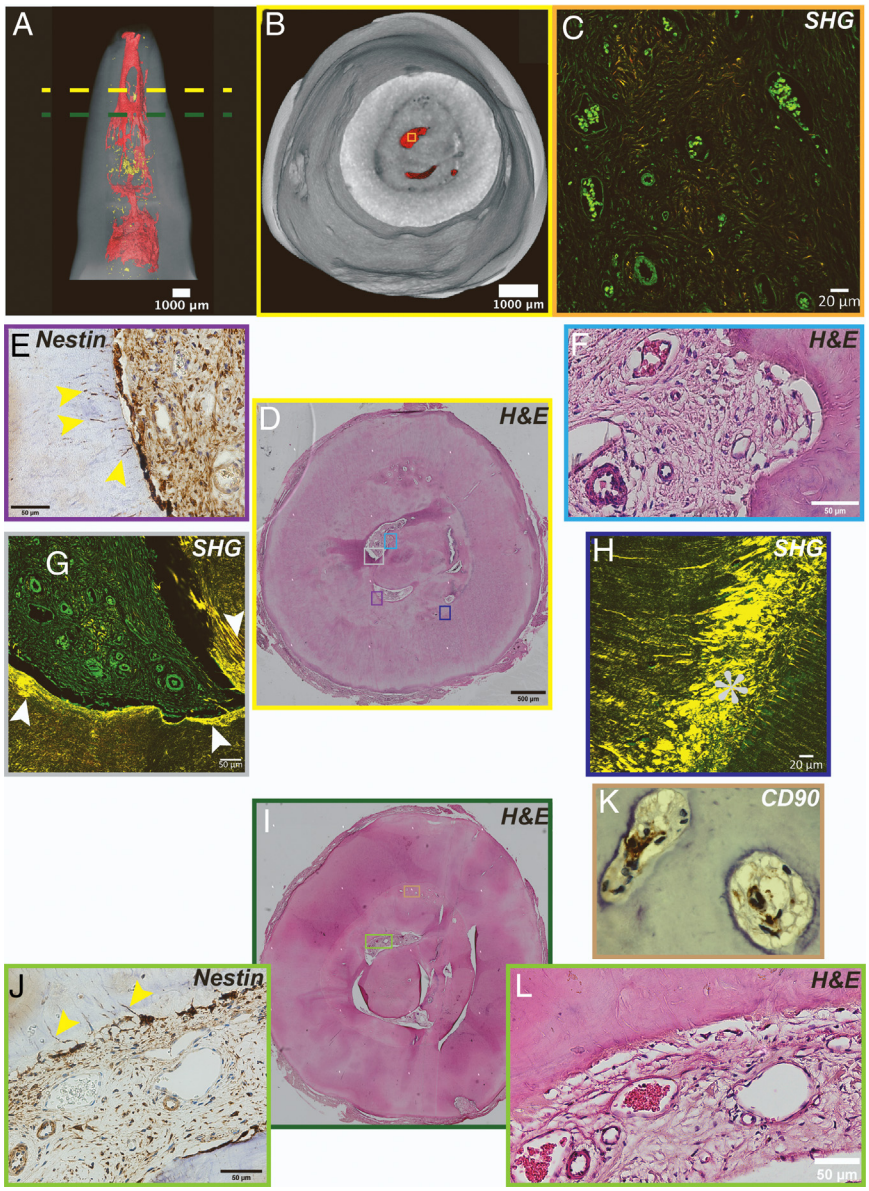

FIGURE 8 – Case 3 (RET), (*A*) 3D reconstruction of the nano-CT scan 3-year post-RET, (*B*) nano-CT cross-section of the root corresponding to the dashed yellow line in (*A*) showing the calciotraumatic line defining hard tissue formation post-RET, (*C*) SHG imaging of the pulp core of an area corresponding to the orange square in (*B*), showing the architecture of the newly formed pulp tissue with several neurovascular bundles and areas of dense collagen I deposition (forward SHG signal in *yellow color*), (*D*) H&E stained cross-section corresponding to (*B*), (*E*) nestin immunostaining for an area corresponding to the purple rectangle in (*D*), showing an odontoblast-like layer with processes extending into the newly formed dentin, (*F*) magnification of the blue rectangle in (*D*) showing a loose connective tissue rich in cells, with cells lining tubular dentin (*yellow arrowhead*), (*G*) SHG of an area corresponding to the gray rectangle in (*D*) showing a dense collagen deposition parallel to the root canal wall (*white arrowheads*), (*H*) SHG of an area corresponding to the blue rectangle in (*D*) showing dense collagen deposition at the transition from primary to newly formed dentin (*white asterisk*), (*I*) H&E stained cross-section corresponding to the dashed green line in (*A*), (*J*) nestin immunostaining for an area corresponding to the green rectangle in (*I*), showing a functional odontoblast-like cell layer with processes extending into the newly formed dentin and a nestin staining pattern very similar to normal, (*K*) magnification of the orange rectangle in (*I*), showing the presence of $CD90^{+}$ cells, (*L*) magnification of the green rectangle in (*I*), showing the architecture of the newly formed tissue. RET, regenerative endodontic treatment; CT, Computed tomography; H&E, hematoxylin and eosin; SHG, Second harmonic generation; TAT, Tooth autotransplantation.

ACKNOWLEDGMENTS

M.E., S.P., L.X., and R.B.D., contributed to the conception, design, data acquisition, analysis, interpretation, drafted and critically revised the manuscript; J.W., G.V.G., N.M, B.V.M., I.L., and R.J., contributed to data acquisition, interpretation, and critically revised the manuscript. All authors gave final approval and agreed to be accountable for all aspects of the study.

The authors would like to thank Prof. Ghislain Opdenakker for his critical reading and for correcting the manuscript. A special thanks to Mr Tobie Martens for his assistance with the SHG imaging and to Dr Kathleen Van den

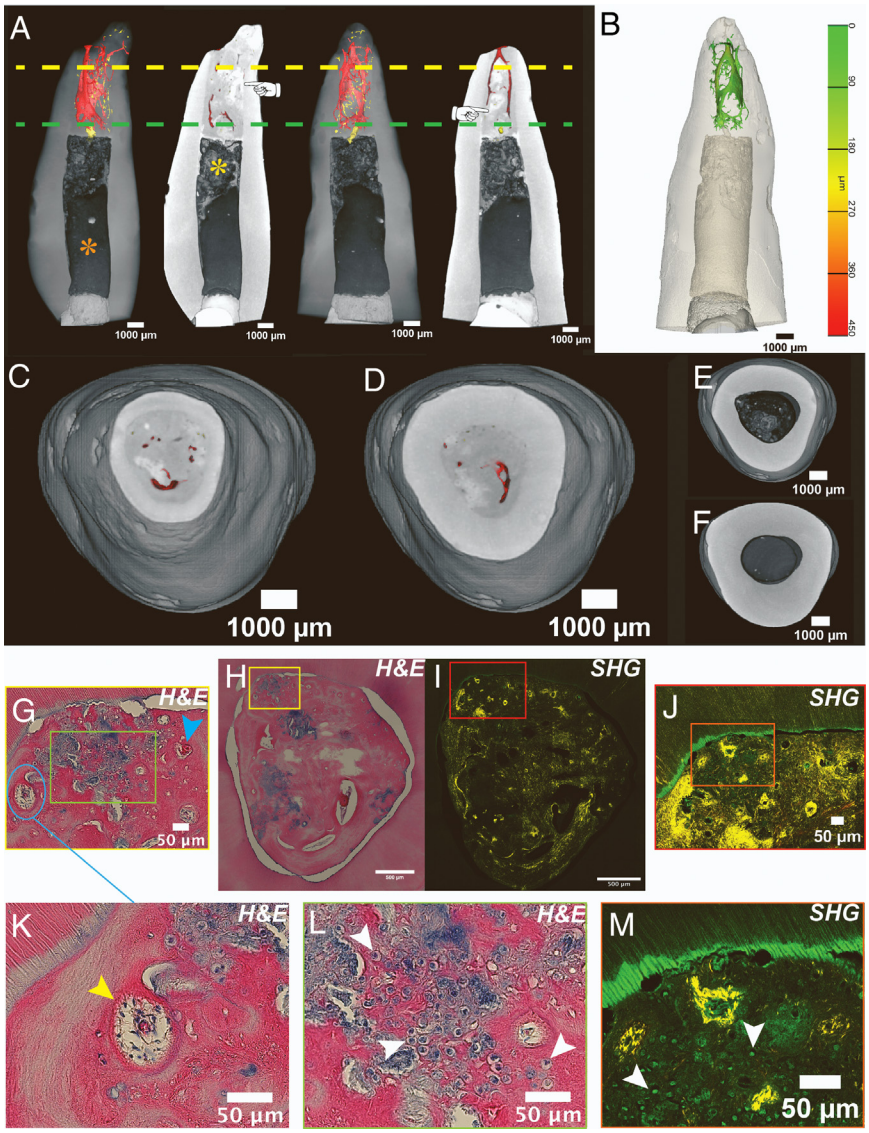

FIGURE 9 – Case 4 (RET), multimodality imaging for the pattern of pulp healing 3 years post-RET, (*A*) 3D reconstruction of tooth #8 from the nano-CT scan 3 year post-RET, note the 3D interconnected root canal system (in *red*) and the porosity inside newly formed tissue (in *yellow*) and longitudinal sections showing the hard tissue formation post-RET showing zones of different intensities and porosities (pointing hands), (*B*) color-coded map for the root canal system thickness (mean = 61.6 µm ± 33.2), (*C*) nano-CT cross-section at the apical third of the root corresponding to the dashed yellow line in (*A*), (*D*) nano-CT cross-section at the apical third of the root corresponding to the dashed green line in (*A*), (*E*) nano-CT cross-section at the zone containing material remnants corresponding to the yellow asterisk in (*A*), (*F*) nano-CT cross-section for the calcium silicate cement corresponding to the orange asterisk in (*A*), (*G*) H&E stained section corresponding to the yellow square in (*H*) showing connective tissue inclusions (*blue circle*) and blood vessel (*blue arrowhead*), (*H*) H&E stained cross-section corresponding to (*C*) showing an overview of the newly formed hard-tissue architecture, (I) SHG for a cross-section corresponding to (*C & H*) demonstrating the highly un-organized nature of the collagen deposition within the newly formed tissue, (*J*) SHG for an area corresponding to the red square in (*I*) further demonstrating the collagen deposition pattern (intense forward SHG signal in *yellow color*), (*K*) magnification for the area within the blue circle in (*G*) showing the connective tissue inclusions (*yellow arrowhead*), (*L*) magnification for the area within the green rectangle in (*G*) showing cellular inclusions within the newly formed tissue (*white arrowheads*), (*M*) magnification for the area within the orange rectangle in (*J*) showing cellular inclusions within the newly formed tissue (*white arrowheads*). RET, Regenerative endodontic treatment; CT, Computed tomography; H&E, Hematoxylin and eosin; SHG, Second harmonic generation; TAT, Tooth autotransplantation.

Eynde and Miss Eef Allegaert for their assistance with the nestin immunostaining.

Images were recorded on a Zeiss LSM 780 – SP Mai Tai HP DS (Cell and Tissue Imaging Cluster (CIC), Supported by Hercules AKUL/11/37 and FWO G.0929.15 to Pieter Vanden Berghe, University of Leuven. This study was supported by the Research Council of KU Leuven (grant number C24/18/068).

The authors declare that the research was conducted without any commercial or financial relationships that could be construed as a potential conflict of interest.

SUPPLEMENTARY MATERIAL

Supplementary material associated with this article can be found in the online version at www.jendodon.com (https://doi.org/10.1016/j.joen.2023.06.003).

REFERENCES

1. Akhlef Y, Schwartz O, Andreasen JO, Jensen SS. Autotransplantation of teeth to the anterior maxilla: a systematic review of survival and success, aesthetic presentation and patient-reported outcome. Dent Traumatol 2018;34:20–7.
2. Andreasen JO, Hjorting-Hansen E. Replantation and autotransplantation of teeth. Trans Int Conf Oral Surg 1970:430–3.
3. Czochrowska EM, Stenvik A, Album B, Zachrisson BU. Autotransplantation of premolars to replace maxillary incisors: a comparison with natural incisors. Am J Orthod Dentofacial Orthop 2000;118:592–600.
4. Denys D, Shahbazian M, Jacobs R, et al. Importance of root development in autotransplantations: a retrospective study of 137 teeth with a follow-up period varying from 1 week to 14 years. Eur J Orthod 2013;35:680–8.
5. Kafourou V, Tong HJ, Day P, et al. Outcomes and prognostic factors that influence the success of tooth autotransplantation in children and adolescents. Dent Traumatol 2017;33:393–9.
6. Andreasen JO, Hjorting-Hansen E. Replantation of teeth. II. Histological study of 22 replanted anterior teeth in humans. Acta Odontol Scand 1966;24:287–306.
7. Gronthos S, Mankani M, Brahim J, et al. Postnatal human dental pulp stem cells (DPSCs) *in vitro* and *in vivo*. Proc Natl Acad Sci U S A 2000;97:13625–30.
8. Andreasen JO, Paulsen HU, Yu Z, Bayer T. A long-term study of 370 autotransplanted premolars. Part IV. Root development subsequent to transplantation. Eur J Orthod 1990;12:38–50.
9. Andreasen JO, Paulsen HU, Yu Z, et al. A long-term study of 370 autotransplanted premolars. Part II. Tooth survival and pulp healing subsequent to transplantation. Eur J Orthod 1990;12:14–24.
10. Andreasen JO, Paulsen HU, Yu Z, Schwartz O. A long-term study of 370 autotransplanted premolars. Part III. Periodontal healing subsequent to transplantation. Eur J Orthod 1990;12:25–37.
11. Shahbazian M, Jacobs R, Wyatt J, et al. Validation of the cone beam computed tomography-based stereolithographic surgical guide aiding autotransplantation of teeth: clinical case-control study. Oral Surg Oral Med Oral Pathol Oral Radiol 2013;115:667–75.
12. Hargreaves KM, Diogenes A, Teixeira FB. Treatment options: biological basis of regenerative endodontic procedures. J Endod 2013;39(3 Suppl):S30–43.
13. Hargreaves KM, Giesler T, Henry M, Wang Y. Regeneration potential of the young permanent tooth: what does the future hold? J Endod 2008;34(7 Suppl):S51–6.
14. Kristerson L, Andreasen JO. Autotransplantation and replantation of tooth germs in monkeys: effect of damage to the dental follicle and position of transplant in the alveolus. Int J Oral Surg 1984;13:324–33.
15. Skoglund A, Hasselgren G, Tronstad L. Oxidoreductase activity in the pulp of replanted and autotransplanted teeth in young dogs. Oral Surg Oral Med Oral Pathol 1981;52:205–9.
16. Skoglund A, Tronstad L. Pulpal changes in replanted and autotransplanted immature teeth of dogs. J Endod 1981;7:309–16.
17. Skoglund A, Tronstad L, Wallenius K. A microangiographic study of vascular changes in replanted and autotransplanted teeth of young dogs. Oral Surg Oral Med Oral Pathol 1978;45:17–28.
18. Lee Y, Go EJ, Jung HS, et al. Immunohistochemical analysis of pulpal regeneration by nestin expression in replanted teeth. Int Endod J 2012;45:652–9.
19. Ohshima H, Nakakura-Ohshima K, Yamamoto H, Maeda T. Alteration in the expression of heat shock protein (hsp) 25-immunoreactivity in the dental pulp of rat molars following tooth replantation. Arch Histol Cytol 2001;64:425–37.
20. Panzarini SR, Okamoto R, Poi WR, et al. Histological and immunohistochemical analyses of the chronology of healing process after immediate tooth replantation in incisor rat teeth. Dent Traumatol 2013;29:15–22.
21. Takamori Y, Suzuki H, Nakakura-Ohshima K, et al. Capacity of dental pulp differentiation in mouse molars as demonstrated by allogenic tooth transplantation. J Histochem Cytochem 2008;56:1075–86.

22. Fiane JE, Breivik M, Vandevska-Radunovic V. A histomorphometric and radiographic study of replanted human premolars. Eur J Orthod 2014;36(6):641–8.

23. EzEldeen M, Van Gorp G, Van Dessel J, et al. 3-dimensional analysis of regenerative endodontic treatment outcome. J Endod 2015;41:317–24.

24. Meschi N, EzEldeen M, Torres Garcia AE, et al. A retrospective case series in regenerative endodontics: trend analysis based on clinical evaluation and 2- and 3-dimensional radiology. J Endod 2018;44:1517–25.

25. Meschi N, Hilkens P, Van Gorp G, et al. Regenerative endodontic procedures posttrauma: immunohistologic analysis of a retrospective series of failed cases. J Endod 2019;45:427–34.

26. Huang GT, Garcia-Godoy F. Missing concepts in de novo pulp regeneration. J Dent Res 2014;93:717–24.

27. Austah O, Joon R, Fath WM, et al. Comprehensive characterization of 2 immature teeth treated with regenerative endodontic procedures. J Endod 2018;44:1802–11.

28. Tirez E, Pedano MS. Regeneration of the pulp tissue: cell homing versus cell transplantation approach: a systematic review. Materials 2022;15:8603.

29. EzEldeen M, Wyatt J, Al-Rimawi A, et al. Use of CBCT guidance for tooth autotransplantation in children. J Dent Res 2019;98:406–13.

30. Kristerson L, Andreasen JO. Influence of root development on periodontal and pulpal healing after replantation of incisors in monkeys. Int J Oral Surg 1984;13:313–23.

31. Sonoyama W, Liu Y, Fang D, et al. Mesenchymal stem cell-mediated functional tooth regeneration in swine. PLoS One 2006;1:e79.

32. Volponi AA, Sharpe PT. The tooth – a treasure chest of stem cells. Br Dent J 2013;215:353–8.

33. Nakakura-Ohshima K, Watanabe J, Kenmotsu S, Ohshima H. Possible role of immunocompetent cells and the expression of heat shock protein-25 in the process of pulpal regeneration after tooth injury in rat molars. J Electron Microsc 2003;52:581–91.

34. Rungvechvuttivittaya S, Okiji T, Suda H. Responses of macrophage-associated antigen-expressing cells in the dental pulp of rat molars to experimental tooth replantation. Arch Oral Biol 1998;43:701–10.

35. Sotirovska Ivkovska A, Zabokova-Bilbilova E, Georgiev Z, et al. Immunohistochemical study on antigen-presenting cells in healthy and carious human teeth. Bratisl Lek Listy 2018;119:249–53.

36. Pedano MS, Li X, Jeanneau C, et al. Survival of human dental pulp cells after 4-week culture in human tooth model. J Dent 2019;86:33–40.

37. Pedano MS, Li X, Camargo B, et al. Injectable phosphopullulan-functionalized calcium-silicate cement for pulp-tissue engineering: an *in-vivo* and *ex-vivo* study. Dent Mater 2020;36:512–26.

38. Téclès O, Laurent P, Aubut V, About I. Human tooth culture: a study model for reparative dentinogenesis and direct pulp capping materials biocompatibility. J Biomed Mater Res B Appl Biomater 2008;85B:180–7.

39. Téclès O, Laurent P, Zygouritsas S, et al. Activation of human dental pulp progenitor/stem cells in response to odontoblast injury. Arch Oral Biol 2005;50:103–8.

40. About I, Laurent-Maquin D, Lendahl U, Mitsiadis TA. Nestin expression in embryonic and adult human teeth under normal and pathological conditions. Am J Pathol 2000;157:287–95.

41. Quispe-Salcedo A, Ida-Yonemochi H, Nakatomi M, Ohshima H. Expression patterns of nestin and dentin sialoprotein during dentinogenesis in mice. Biomed Res 2012;33:119–32.

42. Lei L, Chen Y, Zhou R, et al. Histologic and immunohistochemical findings of a human immature permanent tooth with apical periodontitis after regenerative endodontic treatment. J Endod 2015;41:1172–9.

43. Meschi N, Hilkens P, Lambrichts I, et al. Regenerative endodontic procedure of an infected immature permanent human tooth: an immunohistological study. Clin Oral Investig 2016;20:807–14.

44. Torabinejad M, Faras H. A clinical and histological report of a tooth with an open apex treated with regenerative endodontics using platelet-rich plasma. J Endod 2012;38:864–8.

45. Galler KM, Krastl G, Simon S, et al. European society of endodontology position statement: revitalization procedures. Int Endod J 2016;49:717–23.

46. Chrepa V, Joon R, Austah O, et al. Clinical outcomes of immature teeth treated with regenerative endodontic procedures-a san antonio study. J Endod 2020;46:1074–84.

47. Lui JN, Lim WY, Ricucci D. An immunofluorescence study to analyze wound healing outcomes of regenerative endodontics in an immature premolar with chronic apical abscess. J Endod 2020;46:627–40.

48. Nosrat A, Kolahdouzan A, Hosseini F, et al. Histologic outcomes of uninfected human immature teeth treated with regenerative endodontics: 2 case reports. J Endod 2015;41:1725–9.